Optical frequency comb spectroscopy

A. Foltynowicz,* P. Masłowski,† T. Ban,‡ F. Adler, K. C. Cossel, T. C. Briles and J. Ye*

Received 11th January 2011, Accepted 25th January 2011
DOI: 10.1039/c1fd00005e

Optical frequency combs offer enormous potential in the detection and control of atoms and molecules by combining their vast spectral coverage with the extremely high spectral resolution of each individual comb component. Sensitive and multiplexed trace gas detection *via* cavity-enhanced direct frequency comb spectroscopy has been demonstrated for various molecules and applications; however, previous demonstrations have been confined to the visible and near-infrared wavelength range. Future spectroscopic capabilities are created by developing comb sources and spectrometers for the deep ultraviolet and mid-infrared spectral regions. Here we present a broadband high resolution mid-infrared frequency comb-based Fourier transform spectrometer operating in the important molecular fingerprint spectral region of 2100–3600 cm^{-1} (2.8–4.8 μm). The spectrometer, employing a multipass cell, allows simultaneous acquisition of broadband, high resolution spectra (down to 0.0035 cm^{-1}) of many molecular species at concentrations in the part-per-billion range in less than 1 min acquisition time. The system enables precise measurements of concentration even in gas mixtures that exhibit continuous absorption bands. The current sensitivity, 2×10^{-8} cm^{-1} $Hz^{-1/2}$ per spectral element, is expected to improve by two orders of magnitude with an external enhancement cavity. We have demonstrated this sensitivity increase by combining cavity-enhanced frequency comb spectroscopy with a scanning Fourier transform spectrometer in the near-infrared region and achieving a sensitivity of 4.7×10^{-10} cm^{-1} $Hz^{-1/2}$. A cavity-enhanced mid-infrared comb spectrometer will provide a near real-time, high sensitivity, high resolution, precisely frequency calibrated, broad bandwidth system for many applications.

I. Introduction

The development of optical frequency combs at the turn of the millennium revolutionized many fields of physics.[1,2] The unique combination of large bandwidth and high spectral resolution provided by optical frequency combs makes them suitable not only for precision spectroscopy but also for highly sensitive multi-species detection of molecular constituents in the gas phase. In particular, direct frequency comb spectroscopy (DFCS[3]) can use the entire bandwidth of the mode-locked laser with the resolution limited only by the width of a single comb line, which can range from several kilohertz to sub-hertz.[3–6] The DFCS technique is virtually equivalent to a simultaneous measurement with tens of thousands of narrow laser lines and has the potential to become the ultimate tool for applications such as precision

JILA, National Institute of Standards and Technology and University of Colorado, Department of Physics, University of Colorado, Boulder, CO, 80309-0440, USA. E-mail: aleksandra.matyba@jila.colorado.edu; ye@jila.colorado.edu

† Permanent address: Instytut Fizyki, Uniwersytet Mikołaja Kopernika, ul. Grudziadzka 5, 87-100 Torun, Poland.

‡ Permanent address: Institute of Physics, Bijenicka Cesta 46, Zagreb, Croatia.

spectroscopy, trace gas detection and high-resolution quantum control.[7–9] Moreover, the sensitivity of DFCS can be vastly improved by coupling the frequency comb to a high finesse optical cavity.[10–15]

Frequency combs are produced by femtosecond mode-locked lasers, which emit a regular train of ultrashort pulses in the time domain. Due to the interference of the highly periodic pulses the broad frequency spectrum of a femtosecond laser consists of thousands of equidistant narrow lines, whose separation is equal to the pulse repetition rate, f_r. In general, each comb mode is offset from an exact integer multiple of f_r by the carrier-envelope-offset frequency, f_0, which originates from a pulse-to-pulse phase slip due to dissimilar phase and group velocities in the laser cavity. Thus, the frequency of the nth line of a frequency comb is given by $\nu_n = nf_r + f_0$ and all comb lines can be simultaneously controlled by adjusting f_r and f_0.

The equidistant frequency comb spectrum may be matched to the mode structure of an external cavity by properly adjusting both f_r and f_0.[13,16] However, the cavity free spectral range (FSR) is constant only over a limited range of optical frequencies due to dispersion in the cavity mirrors, which usually prevents simultaneous coupling of the entire frequency comb spectrum into the cavity.[17] In the first demonstration of cavity-enhanced (CE-) DFCS for molecular detection, cavity ringdown was measured using a monochromator to disperse the spectrum and a scanning mirror to deflect the beam so that time-sensitive ringdown events across all spectral channels were recorded on a CCD camera,[11] as is schematically illustrated in Fig. 1(a). Another possible detection scheme involves a comb Vernier spectrometer, in which f_r is intentionally mismatched to the cavity FSR in such a way that only one comb mode is on resonance at a time, as shown in Fig. 1(b), which results in an effective filtering of the original comb.[6] More powerfully, by dithering the comb modes with respect to the cavity modes it is possible to efficiently reduce the influence of the frequency-to-amplitude noise conversion due to the narrow spectral modes of a high finesse cavity. The transmitted spectrum is then resolved with a system employing a virtually imaged phased array (VIPA)[5,18] in combination with a grating cross-disperser and integrated on a 2D camera.[14,15,19] The VIPA is a plane-parallel solid glass etalon, which disperses the frequency comb components with high resolution in the vertical direction. Next, the grating disperses the comb horizontally and the parallel stripes of light are imaged onto a detector array, where each pixel represents a resolution element, as is shown in Fig. 1(c). An alternative detection scheme for DFCS is Fourier transform spectroscopy (FTS), either using a Michelson interferometer with a mechanical stage[20–22] [Fig. 1(d)] or two femtosecond lasers with slightly different repetition rates [Fig. 1(e)], thus mimicking the effect of a fast-scanning delay stage.[23–26] An advantage of FTS over a VIPA-based system is the wide wavelength coverage especially in spectral regions where a VIPA is not available; however, employing FTS for cavity-enhanced DFCS[27,28] implies that the approach based on sweeping the comb across the cavity modes cannot be used. Instead, the comb has to be locked tightly to the cavity in order to ensure constant transmission, which in turn causes frequency-to-amplitude noise conversion and potentially compromises the sensitivity.

The sensitivity of (CE-)DFCS is determined by the signal-to-noise ratio (S/N) in the normalized spectrum, *i.e.* the ratio of the sample and reference spectra. In the case of multi-array detection the signal from all detectors is acquired simultaneously and the S/N is determined by that obtained directly at a single detector in the array. When FTS is used the S/N in the frequency-domain spectrum, $(S/N)_f$, is related to the S/N in the time-domain (interferogram), $(S/N)_t$, as

$$(S/N)_f = (S/N)_t \frac{\sqrt{N}}{M}, \quad (1)$$

where N is the number of data points in the interferogram and M is the number of resolved spectral elements.[29] Since the absorption signal is collected over the entire available spectral range, it is justified to normalize the sensitivity to the number of

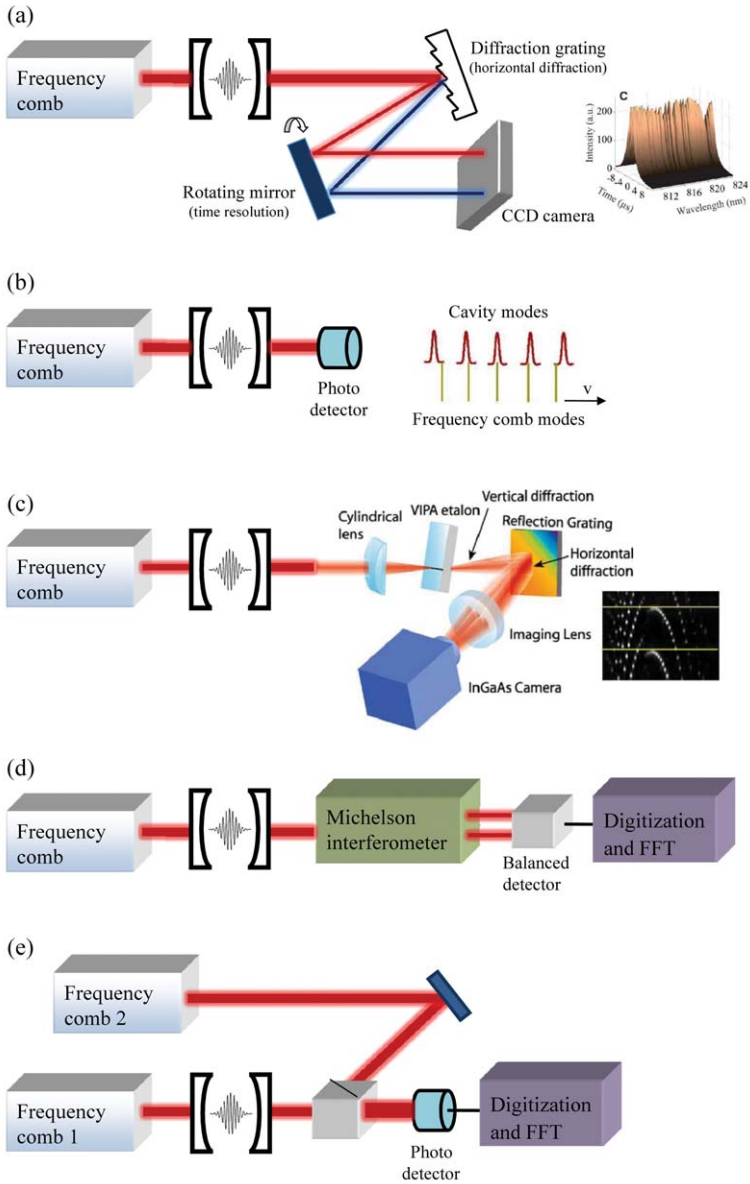

Fig. 1 Possible detection schemes for CE-DFCS. (a) Cavity ringdown measurement using a diffraction grating and a rotating mirror to image the ringdown events onto a CCD camera.[11] (b) The comb Vernier spectrometer in which the laser repetition frequency is detuned from the cavity FSR so that only one comb mode is resonant with the cavity.[6] (c) Frequency comb modes dithered with respect to the cavity modes, the cavity output dispersed with a VIPA and a grating, and integrated on a CCD camera.[14] The horizontal lines on the camera image indicate the FSR of the VIPA. (d) Frequency comb locked tightly to the cavity and the cavity output analyzed with Fourier transform spectrometer. (e) Dual comb approach: one frequency comb locked to a cavity and the cavity output beating on a single detector with a second frequency comb with a slightly different repetition frequency.[27]

resolved spectral elements.[30] The minimum detectable absorption per spectral element is then given by

$$\alpha_{\min} = \left[L_{\text{eff}}(S/N)_{\text{f}}\right]^{-1}\sqrt{\frac{T}{M}} \quad (2)$$

in units of $\text{cm}^{-1}\ \text{Hz}^{-1/2}$, where L_{eff} is the effective interaction length and T the acquisition time of the interferogram.[10,22] This equation is valid also for the multi-array detection scheme (with T being the acquisition time of the entire spectrum and $(S/N)_{\text{f}}$ the inverse of relative noise on a single detector), which also benefits from the multiplex advantage.

For cavity ringdown the effective interaction length is given by FL/π, with L being the cavity length and F the cavity finesse, whereas when the comb is tightly locked to the cavity the enhancement is twice as large, yielding an effective length of $2FL/\pi$. With the sweeping approach the length enhancement factor lies between F/π and $2F/\pi$.[13] Sensitivities obtained with various implementations of CE-DFCS are summarized in Table 1. The second and third columns show the single element sensitivity and sensitivity normalized per spectral element [eqn (2)], respectively. The fourth and fifth columns give the cavity parameters (finesse and length, respectively), and the last two columns show the obtained resolution and spectral bandwidth (together with the center wavelength).

Due to the lack of high-power frequency comb sources in the mid-infrared range, most demonstrations of the (CE-)DFCS technique had to rely on molecular overtone transitions, whose line strengths are on average a factor of 100 weaker than those of fundamental transitions.[11,12] However, the ultrashort pulses of comb sources enable efficient non-linear optical generation of combs in other spectral regions.[19] The first attempts at mid-IR comb spectroscopy, based either on difference frequency generation[24] or an optical parametric oscillator (OPO),[20] did not provide sufficient performance in terms of sensitivity to compete with established techniques. Here we present a high-sensitivity frequency comb Fourier transform spectrometer based on a high power OPO operating in the 2100–3600 cm^{-1} range,[31] where the fundamental frequencies of the C–H and O–H stretching vibrations are located. The spectrometer allows acquisition of broadband molecular spectra with a resolution as high as 0.0035 cm^{-1} and sensitivity of $2 \times 10^{-8}\ \text{cm}^{-1}\ \text{Hz}^{-1/2}$ per spectral element. Due to the high spectral brightness of the frequency comb and the access to strong molecular transitions, gas concentrations at low part-per-billion (ppb)

Table 1 Performance of various cavity-enhanced direct frequency comb spectroscopy implementations: cavity ringdown,[11] VIPA-based detection scheme,[14] dual comb approach,[27] and the near-IR FTS system presented in this work

	Single element sensitivity [cm^{-1}]	Sensitivity per sp. elem. [$\text{cm}^{-1}\ \text{Hz}^{-1/2}$]	Cavity finesse	Cavity length [cm]	Resolution [GHz]	Spectral coverage [nm]
Ref. 11 Fig. 1(a)	6.3×10^{-7} @ 0.15 μs (2.5×10^{-10} @ 1 s)	1.5×10^{-11}	4500	40	24	15 @ 800
Ref. 14 Fig. 1(c)	8×10^{-10} @ 30 s (4.4×10^{-9} @ 1 s)	7.4×10^{-11}	28 000	150	0.8	25 @ 1600
Ref. 27 Fig. 1(e)	1.2×10^{-6} @ 18 μs (4.8×10^{-9} @1 s)	1.0×10^{-10}	1200	230	4.5	20 @ 1040
This work Fig. 1(d)	1.9×10^{-8} @ 6 s (4.7×10^{-8} @ 1 s)	4.7×10^{-10}	8000	60	0.4	30 @ 1530

levels can be measured in a multipass cell in acquisition times under 1 min for various species which are of importance for breath analysis and atmospheric studies.

The use of FTS and a multipass cell in the mid-IR system enables operation over a very broad spectral range.[30] However, the sensitivity is expected to improve by 2 orders of magnitude when the multipass cell is replaced with a high finesse cavity, which would provide part-per-trillion (ppt) level detection limits. Here we also present initial results from an Er:fiber-laser-based system that for the first time efficiently combines a frequency comb tightly locked to an external cavity with FTS as a detection system, reaching a sensitivity of 4.7×10^{-10} cm^{-1} Hz$^{-1/2}$ per spectral element, fully exploiting the cavity enhancement of the interaction length.

II. Mid-infrared frequency comb Fourier transform spectrometry

The mid-IR system is based on an OPO synchronously pumped by a high power Yb:fiber comb with a repetition rate of 136 MHz. The OPO provides up to 1 W of output power with a simultaneous bandwidth of up to 300 cm^{-1} within the 2100–3600 cm^{-1} range.[31] The mid-IR light is coupled into a multipass Herriot cell, in which the total interaction length with the sample is 36.4 m. The light exiting the cell is analyzed with a home-built fast scanning Fourier transform spectrometer. The output of each arm of the Michelson interferometer is measured with two thermoelectrically cooled MCZT (HgCdZnTe) detectors for balanced detection. The optical frequency scale is calibrated using a 780 nm continuous wave (cw) reference laser co-propagating with the mid-IR beam. Both interferograms are recorded using a 22-bit data acquisition board at a rate of 1 MS s^{-1}. The resolution is limited by the maximum optical delay to 0.0035 cm^{-1} (with one scan taking 11 s). Most of the spectra were acquired with 400 MHz (0.013 cm^{-1}) resolution, for which the acquisition time of a single scan is 3 s.

Examples of recorded spectra are shown in Fig. 2. Fig. 2(a) shows a spectrum of the ν_3 band of nitrous oxide, N_2O, around 2200 cm^{-1} at a concentration of 9 ppm in

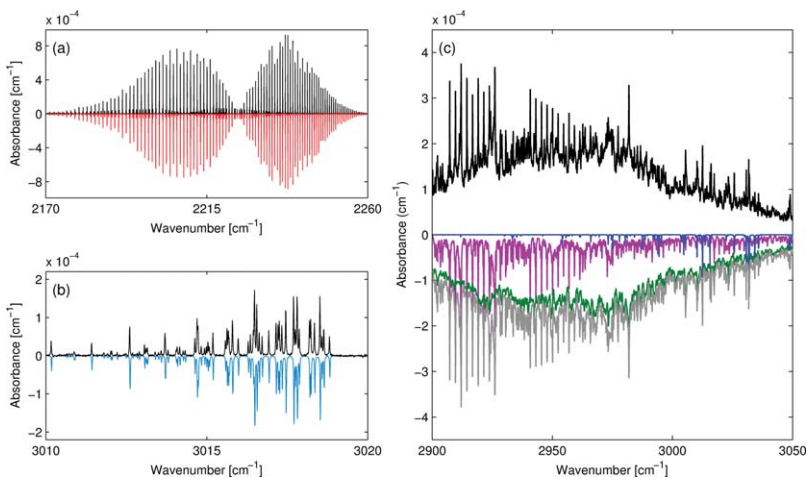

Fig. 2 Examples of spectra acquired with the mid-IR frequency comb-based system. (a) The ν_3 band of 9 ppm of nitrous oxide, N_2O, in 100 Torr of N_2, recorded at a resolution of 0.014 cm^{-1} (black) with a reference spectrum from HITRAN (red), plotted negative for clarity. (b) The Q-branch of 10 ppm of methane, CH_4, at 100 Torr of N_2, at a resolution of 0.0056 cm^{-1} (black) with a reference spectrum from HITRAN (blue), plotted negative for clarity. (c) Spectrum of a mixture of 47 ppm of formaldehyde, H_2CO, 58 ppm of methanol, CH_3OH, and 813 ppm of water, H_2O, in 600 Torr of N_2, at a resolution of 0.014 cm^{-1} (black) and fitted spectra: blue - H_2O from HITRAN, magenta - H_2CO from HITRAN, green - CH_3OH from NWIR, gray - sum of all fits.

100 Torr of N_2. The measured spectrum is plotted in black, and a reference spectrum, calculated using parameters from the HITRAN database,[32] is plotted in red (negative for clarity), proving a good agreement between the experimental and theoretical spectrum. The resolving power of the spectrometer is illustrated in Fig. 2(b), which shows a zoom of the Q-branch of methane, CH_4, around 3000 cm^{-1} measured at a concentration of 10 ppm in 100 Torr of N_2 (black), together with a reference spectrum from HITRAN (blue). Finally, Fig. 2(c) shows a spectrum of a mixture of 47 ppm of formaldehyde, H_2CO, 58 ppm of methanol, CH_3OH, and 813 ppm of water, H_2O, in 600 Torr of N_2 (black). A sum of the spectra of the three molecular constituents was fitted to the data, with gas concentrations as fitting parameters, and the result is shown in gray (negative for clarity). The individual fitted spectra are plotted in blue (H_2O, from HITRAN), magenta (H_2CO, from HITRAN), and green (CH_3OH, from the NWIR database[33]). This example demonstrates that it is possible to extract concentrations of individual species from a measurement of a mixture of several gaseous species even in the presence of molecules with broad spectral features.

The sensitivity of the spectrometer is 2×10^{-8} cm^{-1} $Hz^{-1/2}$ per spectral element, which allows detection of ppb level concentrations of molecules such as methane, ethane, formaldehyde, methanol, nitrous oxide, isoprene, and carbon dioxide, in 30 s (using 400 MHz resolution and 10 averages; 5 averages for sample and background spectra, respectively). In order to improve the sensitivity, an external cavity will be used to enhance the interaction length with the sample. First, though, an initial demonstration of cavity-enhanced frequency comb FTS was accomplished in the near-IR.

III. Cavity-enhanced frequency comb Fourier transform spectrometry

The near-IR system, shown schematically in Fig. 3, is based on an Er:fiber laser with a repetition rate of 250 MHz and a spectrum spanning from 1500 to 1600 nm. The laser is locked to a cavity with a finesse of 8000 and length of 60 cm *via* the Pound-Drever-Hall technique.[34] The light reflected from the cavity is dispersed with a grating and imaged on two detectors, resulting in two error signals centered at two different wavelengths.[35] The feedback is sent to the laser oscillator current and to a fast piezo-electric transducer controlling the laser cavity length. Cavity dispersion limits the transmitted bandwidth to 30 nm centered around 1535 nm. The cavity transmitted light is analyzed with the FTS described above, in which the two MCZT detectors have been replaced with a balanced InGaAs detector.

The main limitation of cavity enhanced spectroscopy utilizing a laser continuously locked to a cavity is usually the noise originating from frequency-to-amplitude noise conversion by the narrow cavity modes. Immunity to this type of noise can be obtained by the use of modulation techniques, as is done for cw lasers in noise-immune cavity-enhanced optical heterodyne molecular spectroscopy (NICE-OHMS).[36,37] The rapid-scan FTS is a modulation technique as well, since the interferogram appears at an audio frequency (around 160 kHz in our case). Thus, the signal is detected at a frequency where the noise is significantly lower than at DC. Moreover, balanced detection efficiently removes the remaining common mode noise, as is illustrated in Fig. 4(a), which shows the cavity transmitted spectrum recorded with one detector (red) and with balanced detection (blue) with 400 MHz resolution during one scan lasting 3 s. Balanced detection reduces the noise by two orders of magnitude; the inset shows a zoom of the cavity transmitted spectrum centered around 6500 cm^{-1}, with a S/N of 240 at the peak of the spectrum. This corresponds to a $(S/N)_f$ of 170 in the normalized spectrum (*i.e.*, in the ratio of two consecutive spectra of cavity filled with reference gas). The minimum detectable absorption is therefore equal to 1.9×10^{-8} cm^{-1} in 6 s acquisition time (3 s for sample and

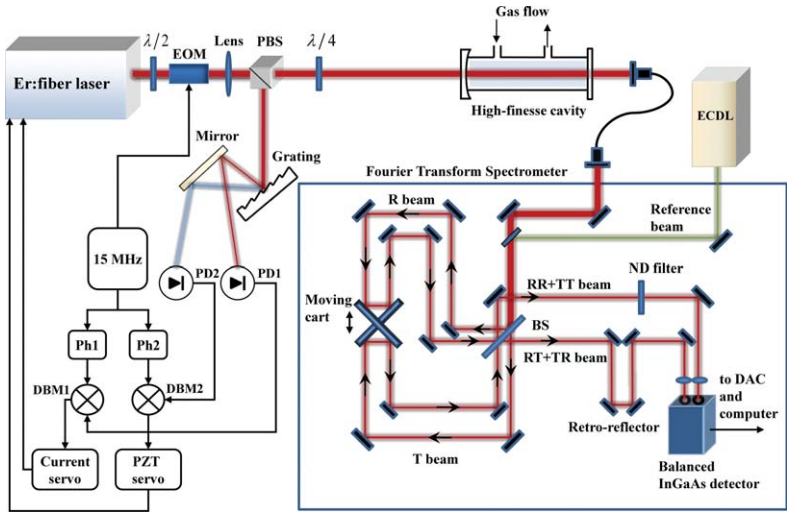

Fig. 3 Schematics of the near-IR CE-DFCS experimental setup. The light from the Er:fiber frequency comb is phase modulated at 15 MHz in an electro-optical modulator (EOM) and incident on a cavity. The cavity reflected light is redirected with a polarizing beam splitter cube (PBS) onto a reflection grating and two photodiodes (PD1 and PD2). The output of both detectors is demodulated at 15 MHz in double balanced mixers (DBM1 and DBM2) in order to produce error signals for laser PZT and current feedback. The light transmitted through the cavity is coupled into a fiber and into a Fourier transforms spectrometer. A reference external cavity diode laser (ECDL) at 780 nm is used for frequency scale calibration. The two interferograms from the FTS are recorded with data acquisition card (DAC) and analyzed on a computer. Other abbreviations: λ/2 - half waveplate, λ/4 - quarter waveplate, Ph - phase shifter, BS - beam splitter, ND - neutral density, R - reflected, and T - transmitted beam.

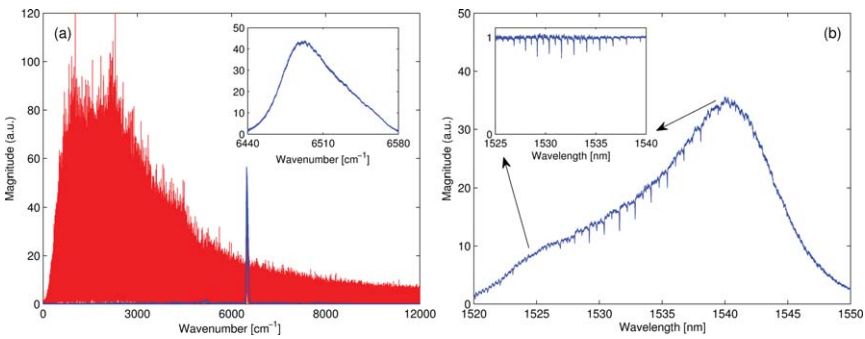

Fig. 4 (a) Spectrum of cavity transmitted light measured with one detector (red) and with balanced detection (blue). The low frequency cut-off is due to the high-pass filter in the detector amplifier. The inset shows a zoom of the cavity transmitted spectrum centered around 6500 cm^{-1}. (b) Spectrum of cavity filled with 1 ppm of acetylene, C_2H_2, in 465 Torr of N_2. The inset shows a zoom of the spectrum normalized to a reference spectrum recorded with a cavity filled with N_2 only.

background spectra, respectively). The cavity transmitted spectrum measured at a resolution of 400 MHz contains 10 000 spectral elements, which yields a sensitivity of 4.7×10^{-10} cm^{-1} $Hz^{-1/2}$ per spectral element. This sensitivity is comparable to that achieved with other CE-DFCS implementations, as was already shown in Table 1. Moreover, preliminary data now suggest that this sensitivity can be improved by at least an order of magnitude. Fig. 4(b) shows a spectrum of the cavity filled

with 1 ppm of acetylene, C_2H_2, at 465 Torr of N_2. The inset displays a zoom of the same spectrum normalized to a reference spectrum. The current sensitivity of the system allows detection of acetylene at concentrations down to tens of ppb level in a few seconds acquisition time.

IV. Conclusions

We have demonstrated the first mid-IR frequency comb-based spectroscopy system capable of detecting ppb level concentrations of various molecules with hundreds of MHz resolution in less than a minute acquisition time. An improvement of sensitivity by up to 2 orders of magnitude is expected when the multipass cell is replaced with a cavity with a finesse of a few thousand, as demonstrated by the initial results from the near-IR system. This would allow detection of various molecules important for applications such as breath analysis and climate studies at part-per-trillion levels in just 30 s. Already in its present configuration, the system provides for the first time a combination of resolution, spectral bandwidth, sensitivity, and acquisition speed that is sufficient for detecting trace quantities of a wide range of molecules under real-world conditions.

Funding support is provided by AFOSR, DTRA, NIST, and NSF. A.F. acknowledges support from the Swedish Research Council, P.M. from the Polish Ministry of Science and Higher Education, T.B. from a Fulbright Fellowship, and K.C.C. from an NSF Graduate Fellowship.

References

1 T. Udem, R. Holzwarth and T. W. Hansch, *Nature*, 2002, **416**, 233.
2 S. T. Cundiff and J. Ye, *Rev. Mod. Phys.*, 2003, **75**, 325.
3 A. Marian, M. C. Stowe, J. R. Lawall, D. Felinto and J. Ye, *Science*, 2004, **306**, 2063.
4 V. Gerginov, C. E. Tanner, S. A. Diddams, A. Bartels and L. Hollberg, *Opt. Lett.*, 2005, **30**, 1734.
5 S. A. Diddams, L. Hollberg and V. Mbele, *Nature*, 2007, **445**, 627.
6 C. Gohle, B. Stein, A. Schliesser, T. Udem and T. W. Hänsch, *Phys. Rev. Lett.*, 2007, **99**, 263902.
7 M. C. Stowe, F. Cruz, A. Marian and J. Ye, *Phys. Rev. Lett.*, 2006, **96**, 153001.
8 M. C. Stowe, A. Pe'er and J. Ye, *Phys. Rev. Lett.*, 2008, **100**, 203001.
9 M. C. Stowe, M. J. Thorpe, A. Pe'er, J. Ye, J. E. Stalnaker, V. Gerginov and S. A. Diddams, *Adv. At., Mol., Opt. Phys.*, 2008, **55**, 1.
10 T. Gherman and D. Romanini, *Opt. Express*, 2002, **10**, 1033.
11 M. J. Thorpe, K. D. Moll, R. J. Jones, B. Safdi and J. Ye, *Science*, 2006, **311**, 1595.
12 M. J. Thorpe, D. D. Hudson, K. D. Moll, J. Lasri and J. Ye, *Opt. Lett.*, 2007, **32**, 307.
13 M. J. Thorpe and J. Ye, *Appl. Phys. B: Lasers Opt.*, 2008, **91**, 397.
14 M. J. Thorpe, D. Balslev-Clausen, M. Kirchner and J. Ye, *Opt. Express*, 2008, **16**, 2387.
15 M. J. Thorpe, F. Adler, K. C. Cossel, M. H. G. de Miranda and J. Ye, *Chem. Phys. Lett.*, 2009, **468**, 1.
16 F. Adler, M. J. Thorpe, K. C. Cossel and J. Ye, *Annu. Rev. Anal. Chem.*, 2010, **3**, 175.
17 M. J. Thorpe, R. J. Jones, K. D. Moll, J. Ye and R. Lalezari, *Opt. Express*, 2005, **13**, 882.
18 M. Shirasaki, *Opt. Lett.*, 1996, **21**, 366.
19 K. C. Cossel, F. Adler, K. A. Bertness, M. J. Thorpe, J. Feng, M. W. Raynor and J. Ye, *Appl. Phys. B: Lasers Opt.*, 2010, **100**, 917.
20 K. A. Tillman, R. R. J. Maier, D. T. Reid and E. D. McNaghten, *Appl. Phys. Lett.*, 2004, **85**, 3366.
21 E. Sorokin, I. T. Sorokina, J. Mandon, G. Guelachvili and N. Picque, *Opt. Express*, 2007, **15**, 16540.
22 J. Mandon, G. Guelachvili and N. Picque, *Nat. Photonics*, 2009, **3**, 99.
23 S. Schiller, *Opt. Lett.*, 2002, **27**, 766.
24 A. Schliesser, M. Brehm, F. Keilmann and D. W. van der Weide, *Opt. Express*, 2005, **13**, 9029.
25 I. Coddington, W. C. Swann and N. R. Newbury, *Phys. Rev. Lett.*, 2008, **100**, 013902.
26 I. Coddington, W. C. Swann and N. R. Newbury, *Phys. Rev. A: At., Mol., Opt. Phys.*, 2010, **82**, 043817.

27 B. Bernhardt, A. Ozawa, P. Jacquet, M. Jacquey, Y. Kobayashi, T. Udem, R. Holzwarth, G. Guelachvili, T. W. Hansch and N. Picque, *Nat. Photonics*, 2010, **4**, 55.
28 S. Kassi, K. Didriche, C. Lauzin, X. de. G. Vaernewijckb, A. Rizopoulos and M. Herman, *Spectrochim. Acta, Part A*, 2010, **75**, 142.
29 N. R. Newbury, I. Coddington and W. C. Swann, *Opt. Express*, 2010, **18**, 7929.
30 F. Adler, P. Maslowski, A. Foltynowicz, K. C. Cossel, T. C. Briles, I. Hartl and J. Ye, *Opt. Express*, 2010, **18**, 21861.
31 F. Adler, K. C. Cossel, M. J. Thorpe, I. Hartl, M. E. Fermann and J. Ye, *Opt. Lett.*, 2009, **34**, 1330.
32 L. S. Rothman, *et al.*, *J. Quant. Spectrosc. Radiat. Transfer*, 2009, **110**, 533.
33 S. W. Sharpe, T. J. Johnson, R. L. Sams, P. M. Chu, G. C. Rhoderick and P. A. Johnson, *Appl. Spectrosc.*, 2004, **58**, 1452.
34 R. W. P. Drever, J. L. Hall, F. V. Kowalski, J. Hough, G. M. Ford, A. J. Munley and H. Ward, *Appl. Phys. B: Photophys. Laser Chem.*, 1983, **31**, 97.
35 R. J. Jones, I. Thomann and J. Ye, *Phys. Rev. A: At., Mol., Opt. Phys.*, 2004, **69**, 051803.
36 J. Ye, L. S. Ma and J. L. Hall, *J. Opt. Soc. Am. B*, 1998, **15**, 6.
37 A. Foltynowicz, F. M. Schmidt, W. Ma and O. Axner, *Appl. Phys. B: Lasers Opt.*, 2008, **92**, 313.